The effects of low temperature on docosahexaenoic acid biosynthesis in *Schizochytrium sp* TIO01 and the underlying mechanism

Fan Hu (fhu2008@foxmail.com)
Ministry of Natural Resources https://orcid.org/0000-0001-9832-2654
April L. Clevenger
University of Oklahoma
Peng Zheng
Wuhan University of Science and Technology
Qiongye Huang
Ministry of Natural Resources
Zhaokai Wang
Ministry of Natural Resources of the People's Republic of China

Research

Keywords: Low temperature, Polyunsaturated fatty acid, Schizochytrium, De novo genome assembly, Differential expression genes

Posted Date: February 3rd, 2020

DOI: https://doi.org/10.21203/rs.2.22487/v1

Version of Record: A version of this preprint was published at Biotechnology for Biofuels on October 16th, 2020. See the published version at https://doi.org/10.1186/s13068-020-01811-y.

Abstract

Background

Schizochytrium are known for their abundant production of docosahexaenoic acid (DHA). Low temperatures can promote the biosynthesis of polyunsaturated fatty acids in many species. In this study, the effects of low temperature on the biosynthesis of DHA in *Schizochytrium* sp TIO01 and the underlying mechanism was investigated.

Results

Based on the de novo genome assembly (contig N50=2.86 Mb) and iTRAQ-based protein identification, we first reconstructed the detailed *Schizochytrium* fatty acid biosynthesis pathway. Our findings revealed that desaturases, involved in DHA synthesis via the fatty acid synthase (FAS) pathway, were completely absent. The polyketide synthase (PKS) pathway and the FAS pathway are separately responsible for DHA and saturated fatty acid synthesis in *Schizochytrium* . Analysis of fatty acid composition profiles indicates that low temperature has a significant impact on the production of DHA in *Schizochytrium*, increasing the DHA content and overall total fatty acids from 43% to 65%. The increased DHA content, however, was not a result of the expression of the PKS pathway genes. Further gene expression analysis indicated that low temperatures may promote DHA accumulation by the up-regulation of both the pentose phosphate pathway and the branched-chain amino acid degradation pathway (increasing the production of the substrates for polyunsaturated fatty acid synthesis: acetyl-CoA and NADPH). In addition, low temerpatures result in a down-regulation of the FAS pathway (reducing the consumption of the substrates for saturated fatty acid synthesis) and malic enzyme, leading to a decreased saturated fatty acid content.

Conclusions

These findings elucidate the detailed fatty acid synthesis pathway of *Schizochytrium*, revealing an underlying mechanism by which low temperatures promote the accumulation of DHA in *Schizochytrium*. The high-quality and nearly complete genome sequence of *Schizochytrium* provides a valuable reference for further investigation of the regulation of polyunsaturated fatty acids biosynthesisand the evolutionary characteristics in *Thraustochytriidae* species.

Background

Docosahexaenoic acid (DHA, C22:6), a major ω-3 polyunsaturated fatty acid (PUFA), is widely distributed among phospholipids in the human brain and retina, playing a vital role in human health [1]. A variety of marine-microorganisms are rich in DHA [2, 3]. As one of the most promising DHA-producing species, Schizochytrium have the ability to accumulate DHA to more than 40% of the total fatty acid (TFA) concentration and ~ 40% of the dry cell weight [4]. On account of this characteristic, the PUFA biosynthesis pathway in Schizochytrium has attracted increasing attention and is currently being exploited by several companies [5].

The entire PUFA synthesis pathway was conventionally considered to occur via two routes: the first is the standard fatty acid synthase (FAS) pathway which involves serial desaturation and elongation of short saturated fatty acids (SSFAs, C16:0 or C18:0). The second includes the polyketide synthase (PKS) pathway [6]. In 2002, Metz et al reported that the PKS pathway is responsible for PUFA synthesis and does not rely on elongation and desaturation of the FAS pathway in Schizochytrium thorugh the use of labeling experiments [7]. This result was subsequently validated by Lippmeier et al, who showed that knock-outs of the PKS gene led to PUFA auxotrophic behavior [8]. Although these biochemical and genetic studies on Schizochytrium have suggested that the PKS pathway is responsible for DHA biosynthesis [7–9], recent studies revealed that enhancement of the FAS pathway contributes significantly to increased DHA productivity in Schizochytrium [10, 11]. Following these results, questions arise as to which route is employed by Schizochytrium for DHA synthesis. Genome sequencing is an ideal approach for investigating this issue, however, information for high-quality whole-genomes for Schizochytrium available in public databases are currently limited [12], preventing the identification of the Schizochytrium PUFA biosynthesis pathway.

Low temperatures have been shown to impact polyunsaturated fatty acid productivity in many PUFA-producing organisms [13–17]. However, few studies have investigated the underlying mechanism of these effects. Ma et al pioneered in-depth studies in Aurantiochytrium, showing that the upregulation of the PKS pathway and downregulation of the FAS pathway play important roles in promoting DHA accumulation [13, 18]. Min et al reported that significant upregulation of the fatty acid desaturases associated with the FAS pathway, leads to PUFA accumulation in Bangia fuscopurpurea [19]. In Shewanella piezotlerans and Photobacterium profundum, upregulation of the PKS pathway genes was not detected despite the increase in PUFA accumulation at a low temperature.[20, 21]. In Schizochytrium, Zeng et al have reported that low temperatures have a significant impact on DHA production, increasing DHA levels of up to 50% of the TFA level [22]. The mechanism underlying this low-temperature-induced DHA accumulation remains unknown in Schizochytrium.

Previously, we isolated a Schizochytrium strain from sea water (designated Schizochytrium sp TIO01)[23]. In this study, the effects of low temperature on fatty acid synthesis in Schizochytrium sp TIO01 was analysis and the underlying mechanism was investigated. Based on the de novo genome assembly and iTRAQ-based LC-MS-MS, we reconstructed the fatty acid biosynthesis pathway of Schizochytrium sp TIO01. Next, the effects of low temperature on fatty acid synthesis was investigated by analysis of differential expression of genes related to fatty acid biosynthesis.

Results

Low temperatures promote Schizochytrium DHA accumulation

Fatty acid composition profiles of Schizochytrium when cultured under both cold and normal temperatures were analyzed. Samples used to analyze fatty acids were cultured and collected at an optical density 650 nm of around 0.7 at 28 °C or 16 °C, as indicated in Fig. 1a. Generally, Schizochytrium sp TIO01 had a similar total lipid content (16° C: 53.53% ± 2.18% (weight/cell dry weight); 28 °C: 51.05% ± 3.05% (weight/cell dry weight)) and lipid content profiles at these

two temperatures. Pentadecanoic acid (C15:0), palmitic acid (C16:0), heptadecanoic acid (C17:0), docosapentaenoic acid (DPA, C22:5, ω-6), and DHA (C22:6, ω-3) were all detected under both conditions. Tetracosanoic acid (C24:0) was detected only when Schizochytrium was cultured at 28 °C. In low temperatures, Schizochytrium exhibited reduced saturated fatty acid biosynthesis and a preference for increased DHA synthesis. DHA constituted ~ 65% of the total fatty acid content at 16 °C compared to ~ 43% at 28 °C (Fig. 1b).

Schizochytrium genome assembly, assessment and annotation

To reveal the fatty acid biosynthesis pathways and further improve our understanding of the underlying mechanism by which low temperatures promote DHA accumulation in Schizochytrium, we performed de novo whole-genome assembly and annotation. Using 13.9 Gb of PacBio RS II subreads (217 × genomic data) and 31 Gb of Illumina PE250 clean data (480 × genomic data), a genome size of 64 Mb with a 45% GC base ratio, containing 34 scaffolds and 3 circular contigs (one of the circular contigs is mtDNA genome which was previously reported [24]) was obtained. The N50 scaffold and N50 contig were 5.83 Mb and 2.86 Mb, respectively. Table 1 shows the detailed information regarding the Schizochytrium assembled genome and the genome for the thraustochytriaceae species. To inspect the de novo assembly accuracy, multiple independent sources of reads were used to assess the assembled genome. Among the 62,457,386 paired Illumina PE250 reads (approximately 480 × coverage of the genome), over 99% could be aligned to the genome. The overall alignment rate of the transcriptomic reads from 14 independent culture conditions (approximately 900 × coverage of the genome) ranged from 95–97%, as shown in Table S1). These results suggested that the Schizochytrium assembled genome was of high-quality and nearly complete. We also evaluated the completeness of the genome assembly using BUSCO-v3.0 (database: eukaryota_odb9) [25]. The results showed that 90.4% of core genes were detected (C: 90.4% [S: 89.1%, D: 1.3%], F: 2.3%, M: 7.3%, 274/303). Based on the integration of RNA-seq data, protein alignment, and de novo predictions, 12,392 protein-coding genes were predicted, with an average transcript size of 1,876.3 bp and a mean of 1.7 exons per gene. In all, 6,796 out of the 12,392 predicted proteins (54.84%) could be classified into families according to their putative functions. The proportions for each database were as follows: KEGG (4,362, 35.20%), SwissProt (5,078, 40.98%), TrEMBL (6,336, 51.13%), Nr (6,063, 48.93%), GO (1,235, 9.97%), and InterPro (6,242, 50.37%).

Table 1
Genome comparison among Thraustochytriaceae species

General features		Schizochytrium TIO01 (This study) (GCA_004764695.1)	Schizochytrium M209059 [12] (GCA_000818945.1)	Aurantiochytrium acetophilum HS399 [26] (GCA_004332575.1)	Aurantiochytrium sp. KH105 [27] (GCA_003116975.1)	Aurantiochytrium sp. T66 [28] (GCA_001462505.1)	Aurantiochyt FCC1311 [29] (GCA_00289
Scaffold	N50	5,831,892	595,797	15,406	367,244	1,342,793	236,568
	L50	4	23	1,036	68	3	47
	N90	1,915,581	144,465	5,607	107,216	115,579	51,606
	L90	12	79	1,770	215	42	177
	Scaf Max length	9,776,036	1,674,554	169,387	1,148,255	19,720,504	1,101,226
	Num of scaffolds	34	322	15,340	215	1,847	2,232
Contig	N50	2,864,487	52,007	13,661	196,455	12,952	22,474
	L50	9	230	1,141	117	894	527
	N90	1,558,441	14,718	1,699	57,189	3,515	5,763
	L90	21	754	5,607	384	3,016	1,792
	Ctg Max length	4,854,459	236,430	169,387	729,578	98,696	129,397
	Num of contigs	67	1,608	15,923	848	6,833	4,504
Other	Plasmids	2	-	-	-	-	-
	Genes	12,392	-	-	-	-	11,520
	Average GC%	44.95%	56.6%	45.19%	57.17%	62.83%	57.13%
	Total BaseNum	64,068,115	39,089,698	59,569,284	76,822,483	43,429,441	38,943,350

iTRAQ-based protein identification

To identify *Schizochytrium* proteins, six samples of *Schizochytrium* cells were grown at both normal temperatures as well as low temperatures and subjected to iTRAQ-based proteomic analysis. Tandem mass spectra were searched against the *Schizochytrium* protein database containing the genomics-predicted proteins and transcriptomics-predicted novel proteins. A total of 4,008 proteins were quantified (Detailed information regarding the iTRAQ identified proteins are shown in **Table S2**), of which 3,196 were annotated by the reference genome and 812 were predicted by transcriptomic analysis. Using KEGG pathway

analysis, 2,939 proteins among the 4,008 were annotated in 45 pathways, these identified proteins are involved in global and overview maps, signal transduction, carbohydrate metabolism, lipid metabolism, amino acid metabolism, energy metabolism among others. The top20 KEGG pathways of iTRAQ identified proteins were shown in **Figure 2a**.

Fatty acid biosynthesis pathway

Based on genome annotations and protein identification, the fatty acid biosynthesis pathways of *Schizochytrium*, including the saturated fatty acids synthesis pathway and the PUFA synthesis pathway were reconstructed (**Figure 3**). Annotations regarding these proteins and their detailed LC-MS-MS information are listed in **Table S3 & Table S2**, respectively.

As shown in **Figure 3**, the FAS pathway and the polyketide synthase (PKS) pathways are separately responsible for saturated fatty acid and PUFA synthesis. There are two principal pathways involved in short saturated fatty acid (SSFA) synthesis in *Schizochytrium*. Similar to fungi which uses type I fatty acid synthase (FAS) to synthesize SSFA, *Schizochytrium* utilizes a single large multifunctional polypeptide to synthesize SSFA, which contains 4,230 amino acids and shares approximately 99% identity with the fatty acid synthase from *Aurantiochytrium mangrovei* (AKV56231.1).

Genes involved in type II fatty acid biosynthesis which utilize a set of discrete monofunctional enzymes are usually found in archaea and bacteria [30]. These genes were annotated, except for 3-hydroxyacyl-ACP dehydratase (FabZ). 3-Hydroxyacyl-ACP dehydratase catalyzes the third step of fatty acid biosynthesis, dehydrating 3-hydroxyacyl-ACP to form trans-2-enoyl-ACP. These results suggest that the type II fatty acid pathway in *Schizochytrium* sp TIO01 is incomplete and that type I FAS is responsible for the synthesis of C16:0 and odd-length short fatty acids (C15:0 and C17:0) [31]. In *Schizochytrium*, the long-chain fatty acid elongation process uses C16:0 as a substrate to synthesize long-chain saturated fatty acid (C24:0). This procedure consists of four sequential reactions—condensation, reduction, dehydration, and reduction. Genes participating in the elongation process were all annotated (**Table S3**).

The entire pathway of polyunsaturated fatty acid (PUFAs) synthesis was conventionally thought to occur via two routes. The first is the fatty acid synthase (FAS) pathway which involves serial desaturation and elongation of saturated fatty acids (C16:0 or C18:0); the second is the polyketide synthase (PKS) pathway [6]. According to *Schizochytrium* genome annotation, we found that the desaturase involved in the FAS pathway for PUFA synthesis was completely absent (the intermediates of PUFA compounds involved in the FAS pathway for PUFA synthesis, such as C16:1, C18:1, C18:2, C18:3, and C20:3, were not detected by GC). This indicates that the FAS pathway for PUFA synthesis in *Schizochytrium* is incomplete and that the PKS pathway is responsible for PUFA synthesis. Similar to other *Thraustochytriidae* species [32], *Schizochytrium* contains three large multifunctional PKS pathway genes, namely, PfaA, PfaB and PfaC. These three genes were highly homologous (>99%) to proteins from another PUFA-producing species *Aurantiochytrium* sp. L-BL10.

Transcriptomic profiling under cold temperatures

To improve the understanding of the mechanism by which low temperatures promote DHA accumulation, transcriptomic analysis was performed on six samples at both normal and lowertemperatures as described previously. The obtained reads represented an average of 207.11 times the *Schizochytrium* genome length. Of these,11,215 expressed genes were detected, including 9,660 genome predicted genes and 1,555 novel predicted genes. A total of 1,546 genes among 11,215 expressed genes were significantly associated with the low-temperature response (|Fold change| >= 2 and adjusted *p-value* <= 0.001), including 1,237 downregulated genes and 309 upregulated genes. Using KEGG pathway analysis，846 of the 1,546 differentially expressed genes were annotated in 45 pathways. These differentially expressed genes were involved in amino acid metabolism, carbohydrate metabolism, lipid metabolism, global and overview maps, signal transduction, the endocrine system, and so on. The top20 KEGG pathways of differentially expressed genes were shown in **Figure 2b.**

Significantly differentially expressed genes involved in fatty acid synthesis

As shown in **Figure 1b**, *Schizochytrium* exhibited reduced saturated fatty acid biosynthesis and a preference for increased DHA synthesis when cultured under cold temperatures. Transcriptomic and q-PCR analysis indicated that genes involved in the FAS pathway responsible for saturated fatty acid synthesis (such as those encoding fatty acid synthase (FAS), long-chain fatty acid elongase (ELO), and very-long-chain 3-oxoacyl-CoA reductase (VLCR)) were significantly downregulated (**Figure 4 & Figure 6a**), which was consistent with the reduced saturated fatty acid (reduced C15:0, C17:0, C24:0 content). However, the production of C16:0 was not affected (**Figure 1b**). Further analysis showed that two genes involved in fatty acid metabolism in mitochondria were significantly regulated (**Figure 4**). One of these genes was encodes enoyl-CoA hydratase (ECHS), which catalyzes the third step of fatty acid synthesis, and was significantly upregulated. The other gene encodes acyl-CoA dehydrogenase (ACADM), which catalyzes the first step of fatty acid degradation, and was significantly downregulated. These findings suggest that fatty acid metabolism in mitochondria plays an important role in C16:0 synthesis and complements the biosynthesis of C16:0 at low temperatures. Although low temperature has a significant impact on the production of DHA, genes involved in the PKS pathway responsible for the biosynthesis of PUFAs were not significantly regulated according to the transcriptomic analysis (**Figure 4**) and q-PCR results (**Figure 6**a). This suggests that the increased DHA content was not a result of the expression of the PKS pathway genes.

Significantly differentially expressed genes associated with glycolysis, the pentose phosphate pathway and the TCA cycle

Glycolysis and the pentose phosphate pathway directly produce the substrates (acetyl-CoA and NADPH) for fatty acid synthesis. When *Schizochytrium* was cultured under cold conditions, genes involved in glycolysis such as those encoding glycolysis hexokinase (HK),6-phosphofructokinase (PFKA), and phosphoglycerate mutase (PGAM) were significantly downregulated (|Fold change| >=2 and adjusted p-value <0.001) (**Figure 4 & Figure 6a**), indicating that the glycolysis pathway was inhibited to some extent under cold stress. This result is consistent with the glucose consumption analysis (**Figure 1a)**. Glucose-6-phosphate 1-dehydrogenase (PGD), which plays a critical role in microbial and algal lipid accumulation [31, 33], is involved in the pentose phosphate pathway and catalyzes the conversion of gluconate-6P to D-ribulose-5P to produce a large amount of NADPH. Our findings show that this enzyme was significantly

upregulated (**Figure 4 & Figure 6a**). These indicatest that a relatively large amount of glucose is degraded via the pentose phosphate pathway in order to produce NADPH for fatty acid biosynthesis at low temperatures.

Most of the genes that participate in the TCA cycle were not significantly regulated at lower temperatures except succinyl-CoA synthetase (LSC). Downregulated succinyl-CoA synthetase reducs the production of the TCA intermediate compound succinate. To compensate, the levels of succinate and the downstream compound malate could be increased by upregulation of Tyr and Ile degradation pathways (**Figure 5**). Malic enzyme (ME) which is responsible for degrading malate and producing NADPH was downregulated in this study. This enzyme has been demonstrated to promote fatty acid production [34]. These results indicated that more of the malate could enter the TCA cylce to produce the acetyl-CoA precursor citrate (**Figure 5**). Although downregulated malic enzyme reduces the production of NADPH, recent studies have shown that the NADPH produced by malic enzyme enters exclusively into the FAS pathway for SFA biosynthesis and is not involved in the PKS pathway for PUFA biosynthesis [35, 36]. Downregulated ME coupled with decreased SFA content was also observed in this study.

Significantly differentially expressed genes involved in branched-chain amino acid metabolism

Amino acid degradation leads to the production of acetyl-CoA which is an important substrate for fatty acid synthesis. According to the results of the differentially expressed genes analysis, low temperatures induced significant regulation of 20 genes involved in branched-chain amino acids degradation (upregulation of 16 and downregulation of 4) (**Figure 5 & Figure 6b**). The four significantly downregulated genes included genes encoding hydroxymethylglutaryl-CoA synthase (HMGCS), acyl-CoA dehydrogenase (ACADM) and ketol-acid reductoisomerase (BCATC). HMGCS catalyzes the reverse reaction of Leu degradation, leading to the consumption of acetyl-CoA. ACADM participates in Ile degradation and fatty acid degradation in mitochondria. There are six copies of ACADM genes in *Schizochytrium*, two of which were significantly downregulated. It is uncertain whether these two downregulated ACADM genes play roles in Ile degradation or in the first reaction of fatty acid degradation in mitochondria (**Figure 4**). Generally, low temperatures enhanced the degradation of branched-chain amino acids leading to increased production of acetyl-CoA and intermediate products of the TCA cycle (fumarate and succinyl-CoA)(**Figure 4 & Figure 5**). Fumarate and succinyl-CoA could further be degraded via the the TCA cycle to produce acetyl-CoA precursor citrate.

Discussion

Schizochytrium are well known in the field of single-cell oil research for their ability to produce the health-benefitting docosahexaenoic acid. However, the PUFA biosynthesis pathway in Schizochytrium has long been controversial [10, 11, 37]. Based on the high-quality genome sequence of Schizochytrium sp TIO01, we found that desaturase involved in the FAS pathway for PUFA synthesis was absent in Schizochytrium sp TIO01, and the FAS pathway and the PKS pathway were separately responsible for SFA and PUFA synthesis. This result was consistent with the previous biochemical and genetic studies on Schizochytrium [7–9]. The PKS pathway responsible PUFA synthesis also exists in other Thraustochytriidae species. In one of the closest relatives of Schizochytrium, Thraustochytrium, desaraturases involved in the FAS pathway for PUFA synthesis were absent and the PKS pathway was found to be responsible for PUFA synthesis, as evidenced by a genomic survey [6], heterologous candidate gene expression [32] and an in vivo feeding experiment [31]. In another close relative, Aurantiochytrium, the PKS pathway and the FAS pathway have been proposed to separately produce PUFAs and SFAs based on fatty acid feeding experiments [35]. Taken together, these results suggest that the PKS pathway, not the FAS pathway, is responsible for PUFA synthesis in Thraustochytriidae.

Low temperature has a significant impact on PUFA accumulation in many organisms which use the PKS pathway to synthesize PUFA. In this study, we found that low temperatures reduced saturated fatty acid biosynthesis and significantly increased DHA synthesis in Schizochytrium. Further, gene expression analysis revealed that FAS pathway genes were downregulated. In contrast, the expression of PKS pathway genes which are responsible for DHA synthesis, did not increase. This suggests that the increased DHA content was not a result of the expression of the PKS pathway genes. This phenomenon, also present in Shewanella piezotlerans and Photobacterium profundum, increased PUFA content under cold conditions and was not the result of overexpression of PKS pathway genes [20, 21]. In one of the closest relatives of Schizochytrium, Aurantiochytrium, Ma et al have reported that the upregulated PKS pathway genes and downregulated FAS pathway play an important role in promoting DHA accumulation [13, 18]. These results suggest that different mechanisms of regulating PUFA synthesis exist in different organisms.

NADPH and acetyl-CoA are generally accepted as the main substrates for fatty acid biosynthesis, and the overexpression of genes involved in the production of NADPH and acetyl-CoA (malic enzyme, glucose-6-phosphate dehydrogenase, acetyl-CoA synthetase, citrate lyase, the pyruvate dehydrogenase complex) or by exogenous supplementation with an acetyl-CoA precursor (citrate, acetate), has been demonstrated to promote fatty acid production [38]. There are two major contributors for NADPH production: glucose-6-phosphate 1-dehydrogenase (PGD) in the oxidative pentose phosphate pathay and malic enzymes. When Schizochytrium was cultured at a low temperature, upregulated glucose-6-phosphate 1-dehydrogenase (PGD) and downregulated malic enzyme were detected. Although downregulated malic enzyme reduces the production of NADPH, recent studies have shown that the NADPH produced by malic enzyme and glucose-6-phosphate 1-dehydrogenase enter the FAS pathway for SFA and the PKS pathway for PUFA biosynthesis seperately [35, 36]. Upregulated glucose-6-phosphate 1-dehydrogenase coupled with increased polyunsaturated fatty acid content and downregulated malic enzyme coupled with decreased saturated fatty acid content were also obseved in this study. In addition, downregulated malic enzyme could reduce malate which enters the transhydrogenase cycle to produce pyruvate, promoting more malate to enter the TCA cylce to produce the acetyl-CoA precursor citrate. These results indicates that more of the NADPH and acetyl-CoA precursor for PUFA synthesis could be produced separately by the upregulated pentose phosphate pathay and downregulated malic enzyme at low temperatures. Glycolysis and branched-chain amino acid degredation pathways directly produce acetyl-CoA. When Schizochytrium was cultured under cold conditions, a relatively large amount of glucose was degraded via the pentose phosphate pathway to produce NADPH for fatty acid biosynthesis at low temperatures. This leads to reduced acetyl-CoA production. However, the upregulated branched-chain amino acid degredation pathway could complement the biosynthesis of acetyl-CoA. In addition, the downregulated FAS pathway decreases the consumption of acetyl-CoA and NADPH, leading to decreased saturated fatty acid content. As a result, a relatively large amount of acetyl-CoA and NADPH will enter the PKS pathway to increase the PUFA

content. Taken together, upregulation of the pentose phosphate pathway and branched-chain amino acid degradation pathway along with downregulation of the FAS pathway and malic enzyme, may play a key role in DHA accumulation in Schizochytrium under low temperatures.

Conclusions

In the present study, multi-omicss approaches were used to investigate the effects of low temperatures on docosahexaenoic acid biosynthesis and the underlying mechanism in Schizochytrium sp TIO01. Our findings revealed that desaturases, involved in the FAS pathway for DHA synthesis, were completely absent. The PKS pathway is responsible for DHA synthesis in Schizochytrium. Upregulation of the pentose phosphate pathway and branched-chain amino acid degradation pathway (increasing the production of the substrates for polyunsaturated fatty acid synthesis: acetyl-CoA and NADPH) along with downregulattion of the FAS pathway and malic enzyme (reducing the consumption of the substrates for saturated fatty acid synthesis, leading to a decreased saturated fatty acid content) may play an important role in the DHA accumulation under cold conditions. These findings elucidate the detailed fatty acid synthesis pathway of Schizochytrium, revealing an underlying mechanism by which low temperatures promote the accumulation of DHA in Schizochytrium. The high-quality and nearly complete genome sequence of Schizochytrium also provides a valuable reference for further investigations on the regulation of PUFA biosynthesis and the evolutionary characteristics in Thraustochytriidae species.

Methods

Growth, glucose consumption, and fatty acid analysis

The *Schizochytrium* sp. TIO01 (CGMCC no. 4603) strain used in this study was isolated previously and deposited in the China General culture Collection Center. Modified YPD medium (glucose 40 g/L, yeast extract 15 g/L, peptone 5 g/L, pH 7.0) with a salinity equivalent to 50% that of seawater was used to culture *Schizochytrium.*

Growth analysis: *Schizochytrium* was cultured overnight at 28 °C in YPD medium and then inoculated into fresh medium at 180 rpm and 28 °C or 16 °C. Samples were collected at certain intervals, and the optical density was analyzed at 650 nm. The Glucose (GO) Assay Kit (Sigma, GAGO20-1KT) was used to analyze the glucose concentration according to the manufacturer's protocol. Samples used to analyze the fatty acids were cultured at 28 °C or 16 °C and collected when the OD_{650} reached approximately 0.7. Total lipid content was extracted from freeze-dried samples according to the Bligh-Dyer method [39] and analyzed by a Agilent 7890B GC instrument with H2 as the carrier gas using a Agilent J&W CP-Sil 88 column (100 m×0.25 mm i.d., 0.2 μm film thickness; Agilent Technologies). Operating conditions were as follows: the injector and detector temperatures were kept at 250°C and 260°C, respectively; the temperature program was as follows: initial temperature 100°C for 5 min,increased at 8°C/min to 180°C and held at this temperature for 9 min, followed by increasing at 1°C/min to 230°C and held at this temperature for 15 min. The carrier gas was H_2, 40 mL/min and the detector gas flows were: H_2, 40 mL/min and air, 400 mL/min. The FAME mix (C4-C24) consisting of fatty acid standards was purchased from Sigma (cat. no. 18919-1AMP).

Genome assembly, prediction, and annotation

Genome sequencing sample preparation: *Schizochytrium* was cultured at 28 °C and 180 rpm and collected when the OD_{650} reached approximately 0.7. Total genomic DNA was extracted and the whole-genome shotgun sequencing was performed using the PacBio RS II or Illumina PE250 sequencing platform at the Beijing Genomic Institute (BGI, Shenzhen, China).

Transcriptomics sample preparation for gene prediction: fourteen samples were cultured in 7 different media at 28 °C or 16 °C (the medium components are shown in Table S4). Harvesting was performed separately when the OD_{650} reached 0.7. Total RNA was extracted and sequencing on each sample was performed on the BGISEQ-500 (PE100) or Illumina platform (PE150) at the BGI, Shenzhen, China.

Genome estimation and assembly: The genome size was estimated based on the 17-mer spectrum using gce-v1.0.0 as a heterozygosity model [40]; Falcon [41] (fc_env_180425) as used to assemble the PacBio long reads multiple times to produce the longest contig N50. A two-step polishing strategy was used to improve accuracy. Initial polishing was performed by Arrow using PacBio long reads, and further corrective polishing was performed by Pilon-v1.22 [42] with highly accurate Illumina PE250 reads. SSPACE-LongRead-v1.1 [43] was used to construct a scaffold using PacBio reads longer than 10,000 bp. Contigs assembled by Platanus-v1.2.4 [44] using Illumina PE250 reads were used to fill the gaps by GMcloser-v1.6.2 [45]. Illumina reads and transcriptomic reads were analyzed by Bowtie2-v3.4.1 [46] and Histat2-v2.10 [47], respectively, to assess genome completeness. BUSCO-v3.0 [25] (database eukaryota_odb9) was used to evaluate the completeness of the genome.

Gene prediction and annotation: MAKER-v3.01.02 [48] was used to predict genes by combining results obtained from *ab initio* prediction (AUGUSTUS-v3.3.1 [49] and SNAP-v2006-07-28 [50]), protein homology search (against protein sequences from the NCBI database: *Aurantiochytrium* sp. FCC1311 (GCA_002897355.1), *Blastocystis hominis* (GCA_000151665.1), *Fistulifera solaris* (GCA_002217885.1), *Achlya hypogyna* (GCA_002081595.1), *Phytophthora parasitic* (GCA_000247585.2), *Thalassiosira pseudonana* (GCA_000149405.2), FGENESH-predicted proteins using *Phaeodactylum tricornutum* parameters were also used as homologous proteins (http://www.softberry.com/berry.phtml?topic=fgenesh&group=programs&subgroup=gfind)), and transcriptomics (transcripts from 14 diverse conditions were generated using Trinity-v2.6.6 de novo assembly [51] and used as EST evidence). Predicted genes were annotated by alignment to the nonredundant protein sequence (Nr), Kyoto Encyclopedia of Genes and Genomes (KEGG), SwissProt, TrEMBL and InterPro databases using the Basic Local Alignment Search Tool (BLAST) -v2.7.1+, with an E-value cutoff of 1E-5. Gene Ontology (GO) terms were assigned to the genes using the BLAST2GO pipeline [52].

iTRAQ labeling, LC-MS/MS and data analysis

iTRAQ labeling and MS/MS: Six samples were cultured in YPD medium at two different temperatures (28 °C and 16 °C). Two samples were collected when the OD_{650} reached 0.7 at 28 °C (28log); two samples were collected when the OD_{650} reached 0.7 at 16 °C (16log); and two samples were collected when the OD_{650} reached 1.4 at 16 °C (16sta). After cell sonication, 100 μg of the proteins was reduced with 10 mM DTT and alkylated with 15 mM iodoacetamide (IAM). Samples were digested at 37 °C with sequencing-grade modified trypsin solution. Desalted peptides were labeled with iTRAQ reagents (6-plex kit, Applied Biosystems, USA) according to the manufacturer's protocol for the 8-plex iTRAQ Kit. Labels 113 and 116 were used to label 16log; 114 and 117 were used to label 16sta; and 115 and 118 were used to label 28log. The iTRAQ-labeled peptide mixture was dissolved and separated into 20 fractions, and each fraction was loaded by an autosampler onto a 2-cm C18 trap column with buffer A (5% ACN, 0.1%, FA, with a linear gradient from 5% to 35%) and buffer B (98% ACN, 0.1% FA) at a flow rate of 300 nL/min, followed by a wash with up to 80% buffer B. Intact peptides were detected in a Thermo Q-Exactive Orbitrap instrument at a resolution of 70,000. The electrospray voltage applied was 1.6 kV. The AGC target was 3e-6 for full MS and 1e-5 for MS2. For MS scans, the m/z scan range was 350 to 2000 Da.

iTRAQ data analysis: MS/MS data were processed using MaxQuant (v. 1.5.3.8). Tandem mass spectra were searched against the *Schizochytrium* protein database, which contains the genomics-predicted proteins and transcriptomics-predicted novel proteins. Enzyme specificity was set as full cleavage by trypsin, with two maximum missed cleavage sites permitted. The precursor and fragment ion mass tolerances were 5 ppm and 0.02 Da, respectively. The precursor charged states allowed ranged from 1 to 5. Carbamidomethylation (Cys), iTRAQ 8plex (K) and iTRAQ 8plex (N-term) were set as fixed modifications, whereas oxidation (Met) and acetylation (protein N-terminal) were set as variable modifications. For all experiments, only unique peptides were considered for protein quantification. The estimated false discovery rate (FDR) thresholds for peptides and proteins were specified at a maximum of 1%. The minimum peptide length was set at 6.

Transcriptomics sample preparation and q-PCR validation

Transcriptomics sample preparation for analyzing gene expression under two different culture conditions: Six samples were cultured at 28 °C and 16 °C in YPD medium. Harvesting was performed when the OD_{650} reached approximately 0.7. Total RNA was extracted and sequencing on each sample was performed on the Illumina platform (PE150) at the BGI, Shenzhen, China. Data were analyzed using the Hisat2-StringTie pipeline [47].

q-PCR validation: RNA was extracted using the TRIzol method followed by DNAse treatment. The Prime Script II 1st Strand cDNA Synthesis Kit (Takara Biotech Co., Ltd., Dalian, China) was used for cDNA synthesis. q-PCR was performed on a CFX Connect real-time system (Bio-Rad) using Bio-Rad SYBR Green, and 18S rRNA was used as an internal standard; The $2^{-\Delta\Delta CT}$ method was used to analyze the results [53]. All primers were designed by Primer3Web (http://bioinfo.ut.ee/primer3/), and sequence information is provided in Table S5.

Abbreviations

ACACA: Acetyl-CoA carboxylase; ACADM: acyl-CoA dehydrogenase; ACCAT: acetyl-CoA C-acetyltransferase; ACP: Acyl carrier protein domain; BCAT: branched-chain amino acid aminotransferase; BCATC: ketol-acid reductoisomerase; BCKDH: 2-oxoisovalerate dehydrogenase E1 component; DBT: 2-oxoisovalerate dehydrogenase E2 component; DH: dehydratase domain; DHA: docosahexaenoic acid; DPA: docosapentaenoic acid; ECHS: enoyl-CoA hydratase; ELO: long-chain fatty acid elongase; ER: enoylreductase domain; FAH: fumarylacetoacetase; FAS: fatty acid synthase; FabF: 3-oxoacyl-ACP synthase II; FabG: 3-oxoacyl-ACP reductase; FabI: enoyl-ACP reductase; FabZ: 3-hydroxyacyl-ACP dehydratase; GCDH: glutaryl-CoA dehydrogenase; HACD: very long-chain (3R)-3-hydroxyacyl-CoA dehydratase; HGD: homogentisate 1,2-dioxygenase; HK: glycolysis hexokinase; HMGCS: hydroxymethylglutaryl-CoA synthase; IVD: isovaleryl-CoA dehydrogenase; KR: ketoacyl reductase domain; KS: beta-ketoacyl-acyl-carrier-protein synthase domain; LEU: 3-isopropylmalate dehydratase; LSC: succinyl-CoA synthetase; MCAT: malonyl-CoA acyl carrier protein transacylase; MCCB: 3-methylcrotonyl-CoA carboxylase beta subunit; ME: malic enzyme; NGS: next generation sequencing; OXCT: 3-oxoacid CoA-transferase; PC: pyruvate carboxylase; PFKA: 6-phosphofructokinase; PGAM: phosphoglycerate mutase; PGD: Glucose-6-phosphate 1-dehydrogenase; PKS: polyketide synthase; PUFA: polyunsaturated fatty acid; PfaA: polyketide synthase subunit A; PfaB: polyketide synthase subunit B; PfaC: polyketide synthase subunit C; SFA: saturated fatty acid; SSFA: short saturated fatty acid; TAT: tyrosine aminotransferase; TECR: trans-2-enoyl-CoA reductase; TFA: total fatty acid; VLCR: very long-chain 3-oxoacyl-CoA reductase; iTRAQ: Isobaric tags for relative and absolute quantitation.

Declarations

Ethics approval and consent to participate

Not applicable.

Consent for publication

Not applicable.

Availability of data and materials

The raw sequencing reads used for genome assembly and annotation have been deposited in the SRA (Sequence Read Archive) database under Bioproject ID PRJNA483186. The Whole Genome Shotgun project has been deposited at DDBJ/ENA/GenBank under the accession SMSO00000000. Transcriptomic data for analysis of differential gene expression under the two conditions have been deposited in the SRA database under Bioproject ID PRJNA517294. Protein LC-MS-MS data have been deposited in the IPRoX database (https://www.iprox.org/) under the identifier IPX0001511000.

Competing interests

The authors declare that they have no competing interests.

Funding

This work was financially supported by the National Natural Science Foundation of China (no. 31700028); Scientific Research Foundation of Third Institute of Oceanography, SOA (no. 2016008); Natural Science Foundation of Fujian Province (no. 2016J05100).

Author contributions

Fan Hu designed the study and analyzed the NGS data; Peng Zheng performed the iTRAQ analysis; Qiongye Huang prepared the samples and performed the biochemical analysis; Fan Hu, April L. Clevenger and Zhaokai Wang wrote the manuscript. All the authors have read and approved the final version.

Acknowledgments

The authors would like to thank Dr. Xuanmin Guang (BGI, Shenzhen, China) for his helpful advice on NGS data analysis.

Authors' information

Fan Hu: fhu2008@foxmail.com; Third Institute of Oceanography, Ministry of Natural Resources, Xiamen, 361005, China

April L. Clevenger: april.l.clevenger-1@ou.edu; Department of Chemistry and Biochemistry, University of Oklahoma, Norman, Oklahoma, USA

Peng Zheng: pengzh1984@wust.edu.cn; College of Life Science and Healthy, Wuhan University of Science and Technology, Wuhan 430065, China

Qiongye Huang: huangqiongye@qq.com; Third Institute of Oceanography, Ministry of Natural Resources, Xiamen, 361005, China

Zhaokai Wang*: wang@tio.org.cn; Third Institute of Oceanography, Ministry of Natural Resources, Xiamen, 361005, China

References

1. Innis SM. **Dietary omega 3 fatty acids and the developing brain**. *Brain research.* 2008; **1237**:35.
2. Ward OP, Singh A. **Omega-3/6 fatty acids: alternative sources of production**. *Process Biochemistry.* 2005; **40**(12):3627.
3. Gao M, Song X, Feng Y, Li W, Cui Q: **Isolation and characterization of *Aurantiochytrium* species: high docosahexaenoic acid (DHA) production by the newly isolated microalga, *Aurantiochytrium* sp. SD116**. *J Oleo Sci.* 2013; **62**(3):143.
4. Barclay WR. **Fermentation process for producing long chain omega-3 fatty acids with euryhaline microorganisms**. In.: Google Patents; 2002.
5. Marchan LF, Chang KJL, Nichols PD, Mitchell WJ, Polglase JL, Gutierrez T. **Taxonomy, ecology and biotechnological applications of thraustochytrids: A review**. *Biotechnology advances.* 2018; **36**(1):26.
6. Zhao X, Dauenpen M, Qu C, Qiu X. **Genomic analysis of genes involved in the biosynthesis of very long chain polyunsaturated fatty acids in Thraustochytrium sp. 26185**. *Lipids.* 2016; **51**(9):1065.
7. Metz JG, Roessler P, Facciotti D, Levering C, Dittrich F, Lassner M, Valentine R, Lardizabal K, Domergue F, Yamada A. **Production of polyunsaturated fatty acids by polyketide synthases in both prokaryotes and eukaryotes**. *Science.* 2001; **293**(5528):290.
8. Lippmeier JC, Crawford KS, Owen CB, Rivas AA, Metz JG, Apt KE. **Characterization of both polyunsaturated fatty acid biosynthetic pathways in *Schizochytrium* sp**. *Lipids.* 2009; **44**(7):621.
9. Hauvermale A, Kuner J, Rosenzweig B, Guerra D, Diltz S, Metz JG. **Fatty acid production in *Schizochytrium* sp.: Involvement of a polyunsaturated fatty acid synthase and a type I fatty acid synthase**. *Lipids.* 2006; **41**(8):739.
10. Chen W, Zhou P-p, Zhang M, Zhu YM, Wang XP, Luo XA, Bao ZD, Yu LJ. **Transcriptome analysis reveals that up-regulation of the fatty acid synthase gene promotes the accumulation of docosahexaenoic acid in *Schizochytrium* sp. S056 when glycerol is used**. *Algal research.* 2016;**15**:83.
11. Hoang MH, Nguyen C, Pham HQ, Van Nguyen L, Hai TN, Ha CH, Dai Nhan L, Anh HTL, Quynh HTH, Ha NC. **Transcriptome sequencing and comparative analysis of *Schizochytrium mangrovei* PQ6 at different cultivation times**. *Biotechnology letters.* 2016; **38**(10):1781.
12. Ji XJ, Mo KQ, Ren LJ, Li GL, Huang JZ, Huang H. **Genome Sequence of *Schizochytrium* sp. CCTCC M209059, an Effective Producer of Docosahexaenoic Acid-Rich Lipids**. *Genome Announc.* 2015; **3**(4).
13. Ma Z, Tan Y, Cui G, Feng Y, Cui Q, Song X. **Transcriptome and gene expression analysis of DHA producer *Aurantiochytrium* under low temperature conditions**. *Scientific reports.* 2015; **5**:14446.
14. Zhou PP, Lu MB, Li W, Yu LJ. **Microbial production of docosahexaenoic acid by a low temperature adaptive strain *Thraustochytriidae* sp. Z105: screening and optimization**. *Journal of basic microbiology.* 2010; **50**(4):380
15. Aussant J, Guihéneuf F, Stengel DB. **Impact of temperature on fatty acid composition and nutritional value in eight species of microalgae**. *Applied microbiology and biotechnology.* 2018;1.
16. Li J, Ren LJ, Sun GN, Qu L, Huang H. **Comparative metabolomics analysis of docosahexaenoic acid fermentation processes by *Schizochytrium* sp. under different oxygen availability conditions**. *Omics : a journal of integrative biology.* 2013; **17**(5):269.
17. Ren LJ, Feng Y, Li J, Qu L, Huang H. **Impact of phosphate concentration on docosahexaenoic acid production and related enzyme activities in fermentation of Schizochytrium sp**. *Bioprocess Biosyst Eng.* 2013; **36**(9):1177.

18. Ma Z, Tian M, Tan Y, Cui G, Feng Y, Cui Q, Song X. **Response mechanism of the docosahexaenoic acid producer *Aurantiochytrium* under cold stress**. *Algal Research.* 2017; **25**:191.
19. Cao M, Wang D, Mao Y, Kong F, Bi G, Xing Q, Weng Z: **Integrating transcriptomics and metabolomics to characterize the regulation of EPA biosynthesis in response to cold stress in seaweed *Bangia fuscopurpurea***. *Plos One.* 2017; **12**(12):e0186986.
20. Allen EE, Bartlett DH. **Structure and regulation of the omega-3 polyunsaturated fatty acid synthase genes from the deep-sea bacterium Photobacterium profundum strain SS9**. *Microbiology.* 2002; **148**(6):1903.
21. Wang F, Xiao X, Ou HY, Gai Y, Wang F. **Role and regulation of fatty acid biosynthesis in the response of *Shewanella piezotolerans* WP3 to different temperatures and pressures**. *Journal of bacteriology.* 2009; **191**(8):2574.
22. Zeng Y, Ji XJ, Lian M, Ren LJ, Jin LJ, Ouyang PK, Huang H. **Development of a temperature shift strategy for efficient docosahexaenoic acid production by a marine fungoid protist, *Schizochytrium* sp. HX-308**. *Applied biochemistry and biotechnology.* 2011; **164**(3):249.
23. Cheng RB, Lin XZ, Wang ZK, Yang SJ, Rong H, Ma Y. **Establishment of a transgene expression system for the marine microalga *Schizochytrium* by 18S rDNA-targeted homologous recombination**. *World Journal of Microbiology and Biotechnology.* 2011; **27**(3):737.
24. Wang Z, Lou S, Hu F, Wu P, Yang L, Li H, He L, Lin X. **Complete mitochondrial genome of a DHA-rich protist *Schizochytrium* sp. TIO1101**. *Mitochondrial DNA Part B.* 2016; **1**(1):126.
25. Simao FA, Waterhouse RM, Ioannidis P, Kriventseva EV, Zdobnov EM. **BUSCO: assessing genome assembly and annotation completeness with single-copy orthologs**. *Bioinformatics.* 2015; **31**(19):3210.
26. Ganuza E, Yang S, Amezquita M, Giraldo-Silva A, Andersen RA. **Genomics, Biology and Phylogeny *Aurantiochytrium acetophilum* sp. nov. (*Thraustrochytriaceae*), Including First Evidence of Sexual Reproduction**. *Protist.* 2019; **170**(2):209.
27. Iwasaka H, Koyanagi R, Satoh R, Nagano A, Watanabe K, Hisata K, Satoh N, Aki T. **A Possible Trifunctional β-Carotene Synthase Gene Identified in the Draft Genome of *Aurantiochytrium* sp. Strain KH105**. *Genes.* 2018; **9**(4):200.
28. Liu B, Ertesvåg H, Aasen IM, Vadstein O, Brautaset T, Heggeset TMB: **Draft genome sequence of the docosahexaenoic acid producing thraustochytrid *Aurantiochytrium* sp. T66**. *Genomics data.* 2016; **8**:115.
29. Seddiki K, Godart F, Cigliano RA, Sanseverino W, Barakat M, Ortet P, Rébeillé F, Maréchal E, Cagnac O, Amato A. **Sequencing, de novo assembly, and annotation of the complete genome of a new *Thraustochytrid* species, strain CCAP_4062/3**. *Genome Announc.* 2018; **6**(11):e01335.
30. Jenke-Kodama H, Sandmann A, Müller R, Dittmann E. **Evolutionary implications of bacterial polyketide synthases**. *Molecular biology and evolution.* 2005; **22**(10):2027.
31. Zhao X, Qiu X. **Analysis of the biosynthetic process of fatty acids in *Thraustochytrium***. *Biochimie.* 2018; **144**:108.
32. Meesapyodsuk D, Qiu X. **Biosynthetic mechanism of very long chain polyunsaturated fatty acids in *Thraustochytrium* sp. 26185**. *Journal of lipid research.* 2016;jlr. M070136.
33. Xue J, Balamurugan S, Li DW, Liu YH, Zeng H, Wang L, Yang WD, Liu JS, Li HY: **Glucose-6-phosphate dehydrogenase as a target for highly efficient fatty acid biosynthesis in microalgae by enhancing NADPH supply**. *Metabolic engineering.* 2017; **41**:212.
34. Zhang Y, Adams IP, Ratledge C. **Malic enzyme: the controlling activity for lipid production? Overexpression of malic enzyme in *Mucor circinelloides* leads to a 2.5-fold increase in lipid accumulation**. *Microbiology.* 2007; **153**(7):2013.
35. Song X, Tan Y, Liu Y, Zhang J, Liu G, Feng Y, Cui Q. **Different impacts of short-chain fatty acids on saturated and polyunsaturated fatty acid biosynthesis in *Aurantiochytrium* sp. SD116**. *J Agric Food Chem.* 2013; **61**(41):9876.
36. Liu B, Liu J, Sun P, Ma X, Jiang Y, Chen F. **Sesamol enhances cell growth and the biosynthesis and accumulation of docosahexaenoic acid in the microalga *Crypthecodinium cohnii***. *J Agr Food Chem.* 2015; **63**(23):5640.
37. Zhao B, Li Y, Li C, Yang H, Wang W. **Enhancement of *Schizochytrium* DHA synthesis by plasma mutagenesis aided with malonic acid and zeocin screening**. *Applied microbiology and biotechnology.* 2018; **102**(5):2351.
38. Sun XM, Ren LJ, Zhao QY, Ji XJ, Huang H. **Enhancement of lipid accumulation in microalgae by metabolic engineering**. *Biochimica et Biophysica Acta (BBA)-Molecular and Cell Biology of Lipids.* 2019;1864(3):552;
39. Bligh EG, Dyer WJ. **A rapid method of total lipid extraction and purification**. *Can J Biochem Physiol.* 1959; **37**(8):911.
40. Liu B, Shi Y, Yuan J, Hu X, Zhang H, Li N, Li Z, Chen Y, Mu D, Fan W. **Estimation of genomic characteristics by analyzing k-mer frequency in *de novo* genome projects**. *arXiv preprint arXiv:13082012* 2013.
41. Chin CS, Peluso P, Sedlazeck FJ, Nattestad M, Concepcion GT, Clum A, Dunn C, O'Malley R, Figueroa-Balderas R, Morales-Cruz A *et al*. **Phased diploid genome assembly with single-molecule real-time sequencing**. *Nature methods.* 2016; **13**(12):1050.
42. Walker BJ, Abeel T, Shea T, Priest M, Abouelliel A, Sakthikumar S, Cuomo CA, Zeng Q, Wortman J, Young SK *et a*. **Pilon: an integrated tool for comprehensive microbial variant detection and genome assembly improvement**. *Plos One.* 2014; **9**(11):e112963.
43. Boetzer M, Pirovano W. **SSPACE-LongRead: scaffolding bacterial draft genomes using long read sequence information**. *BMC bioinformatics.* 2014; **15**:211.
44. Kajitani R, Toshimoto K, Noguchi H, Toyoda A, Ogura Y, Okuno M, Yabana M, Harada M, Nagayasu E, Maruyama H *et al*. **Efficient de novo assembly of highly heterozygous genomes from whole-genome shotgun short reads**. *Genome Res.* 2014; **24**(8):1384.
45. Kosugi S, Hirakawa H, Tabata S. **GMcloser: closing gaps in assemblies accurately with a likelihood-based selection of contig or long-read alignments**. *Bioinformatics.* 2015; **31**(23):3733.
46. Langmead B, Salzberg SL. **Fast gapped-read alignment with Bowtie 2**. *Nature methods* 2012, **9**(4):357.

47. Pertea M, Kim D, Pertea GM, Leek JT, Salzberg SL. **Transcript-level expression analysis of RNA-seq experiments with HISAT, StringTie and Ballgown**. *Nature protocols.* 2016; **11**(9):1650.
48. Holt C, Yandell M. **MAKER2: an annotation pipeline and genome-database management tool for second-generation genome projects**. *BMC bioinformatics* 2011, **12**(1):491.
49. Stanke M, Diekhans M, Baertsch R, Haussler D: **Using native and syntenically mapped cDNA alignments to improve de novo gene finding**. *Bioinformatics* 2008, **24**(5):637-644.
50. Korf I. **Gene finding in novel genomes**. *BMC bioinformatics.* 2004; **5**(1):59.
51. Grabherr MG, Haas BJ, Yassour M, Levin JZ, Thompson DA, Amit I, Adiconis X, Fan L, Raychowdhury R, Zeng Q. **Full-length transcriptome assembly from RNA-Seq data without a reference genome**. *Nature biotechnology.* 2011; **29**(7):644.
52. Conesa A, Götz S, García-Gómez JM, Terol J, Talón M, Robles M. **Blast2GO: a universal tool for annotation, visualization and analysis in functional genomics research**. *Bioinformatics.* 2005; **21**(18):3674.
53. Xiong Q, Feng J, Li ST, Zhang GY, Qiao ZX, Chen Z, Wu Y, Lin Y, Li T, Ge F *et al.* **Integrated transcriptomic and proteomic analysis of the global response of *Synechococcus* to high light stress**. *Molecular & cellular proteomics: MCP.* 2015; **14**(4):1038.

Supplementary Materials

Table S1 Summary of data and reads alignments used in genome assembly and assessment

Table S2 Detailed information regarding the iTRAQ identified proteins

Table S3 List of predicted genes involved in fatty acid synthesis

Table S4 Constitution of mediums used in RNA_seq samples preparation for protein-coding genes prediction

Table S5 List of q-PCR primer sequences used in this study

Figures

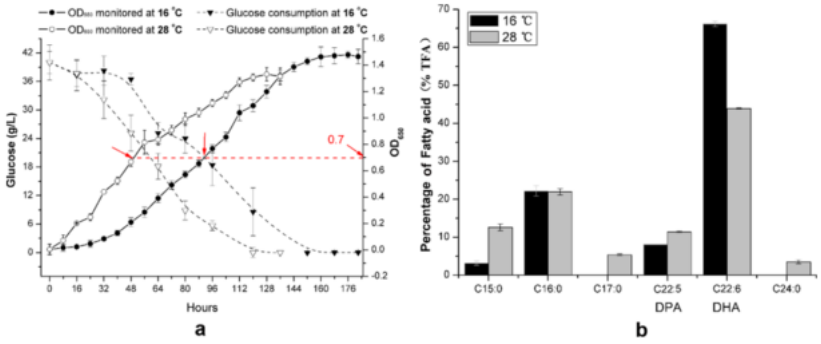

Figure 1

Growth curve (a), glucose consumption (a), and total fatty acid analysis (b) when Schizochytrium was cultured under two different temperatures. (a): Time course analysis of Schizochytrium growth and glucose consumption. The arrows indicate samples collected for subsequent total fatty acid (TFA) analysis and gene expression analysis. (b): Analysis of the TFA composition of Schizochytrium. Abbreviations: DHA: docosahexaenoic acid; DPA: docosapentaenoic acid.

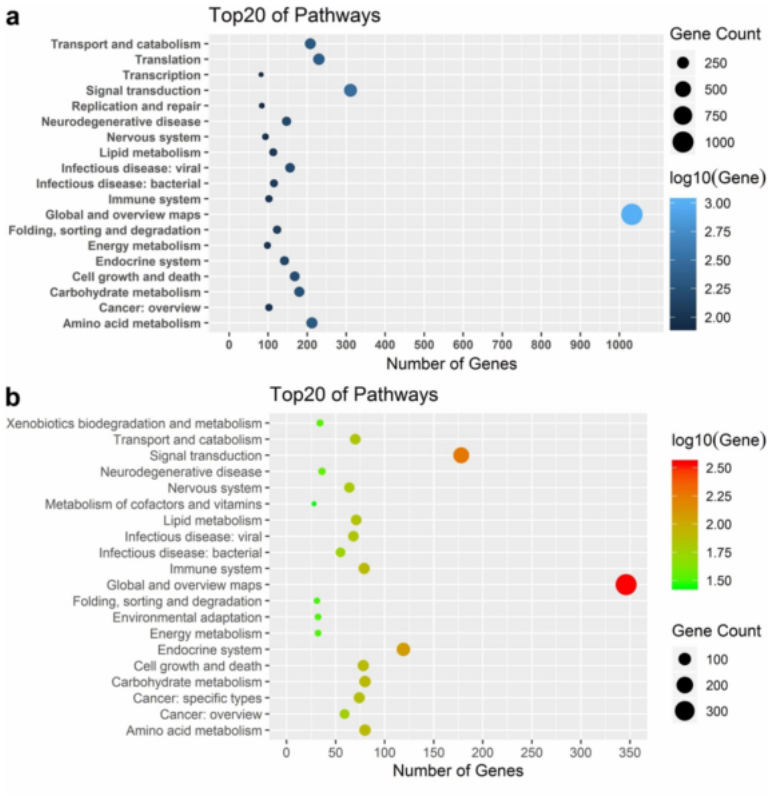

Figure 2

The top 20 KEGG pathways of ITRAQ identified proteins (a) and the top 20 KEGG pathways of differentially expressed genes (b).

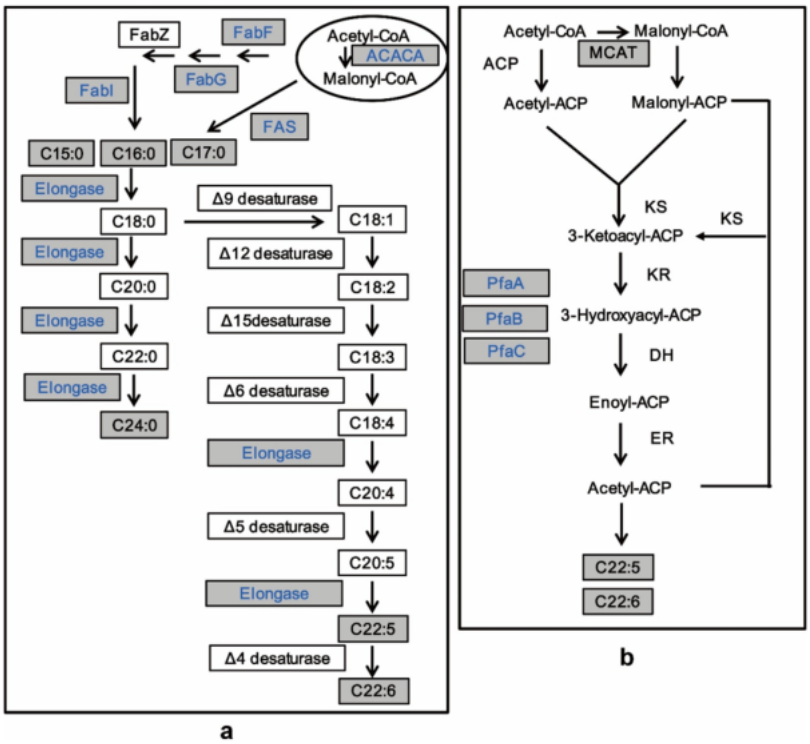

Figure 3

Reconstruction of the fatty acid synthase (FAS, a) and polyketide synthase (PKS, b) pathways in Schizochytrium. Shaded boxes show proteins/fatty acids detected from genome annotations/GC analysis; White boxes indicate proteins/fatty acids not detected. Proteins that were identified by iTRAQ are indicated in blue. Abbreviations: ACACA: Acetyl-CoA carboxylase; FAS: fatty acid synthase; FabF: 3-oxoacyl-ACP synthase II; FabG:3-oxoacyl-ACP reductase; FabI: enoyl-ACP reductase; Elongase contains four enzymes: long-chain fatty acid elongase (ELO), very long-chain 3-oxoacyl-CoA reductase (VLCR), very long-chain (3R)-3-hydroxyacyl-CoA dehydratase (HACD) and trans-2-enoyl-CoA reductase (TECR). PfaA: polyketide synthase subunit A; PfaB: polyketide synthase subunit

B; PfaC: polyketide synthase subunit C; ACP: Acyl carrier protein domain; MCAT: malonyl-CoA acyl carrier protein transacylase; KS: beta-ketoacyl-acyl-carrier-protein synthase domain; KR: ketoacyl reductase domain; DH: dehydratase domain; ER: enoylreductase domain.

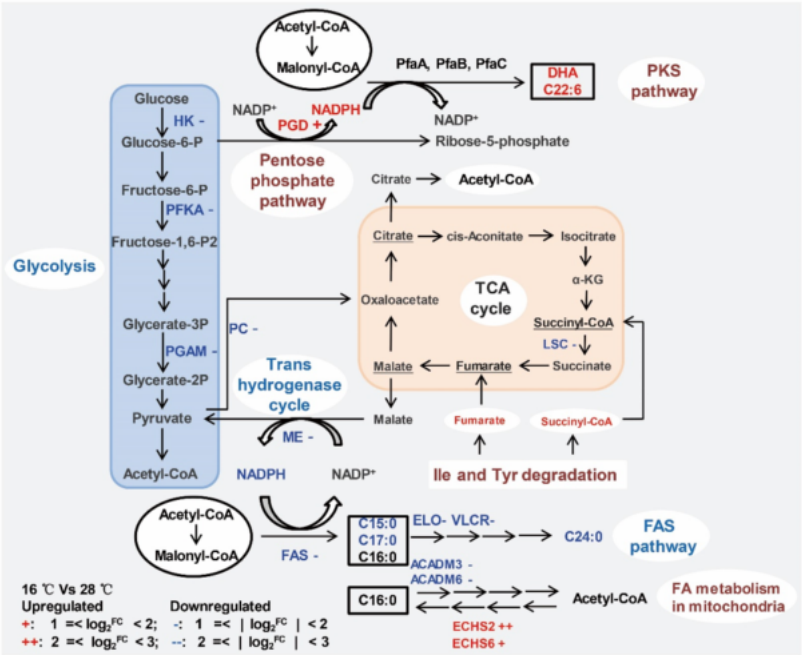

Figure 4

Diagrammatic representation for significantly differentially expressed genes associated with the fatty acid biosynthesis pathways, glycolysis, pentose phosphate and TCA cycle when Schizochytrium was cultured under cold conditons. Genes that were differentially regulated (|Fold change| >=2 and adjusted p-value <0.001) when Schizochytrium was cultured at 16 °C are indicated in red (upregulated) and blue (downregulated). Abbreviations: HK: glycolysis hexokinase; PFKA: 6-phosphofructokinase; PGAM: phosphoglycerate mutase; PC: pyruvate carboxylase; PGD: Glucose-6-phosphate 1-dehydrogenase; PfaA: polyketide synthase subunit A; PfaB: polyketide synthase subunit B; PfaC: polyketide synthase subunit C; ME: malic enzyme; FAS: fatty acid synthase; ELO: long-chain fatty acid elongase; VLCR: very long-chain 3-oxoacyl-CoA reductase; ACADM: acyl-CoA dehydrogenase; ECHS: enoyl-CoA hydratase. LSC: succinyl-CoA synthetase.

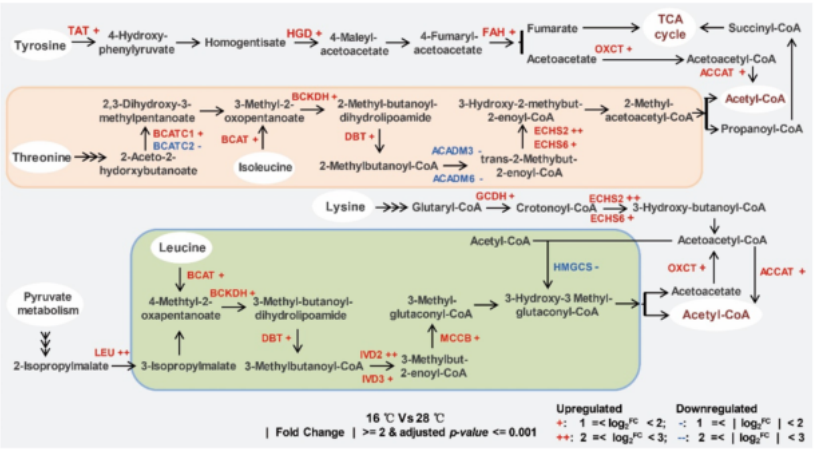

Figure 5

Diagrammatic representation of significantly differentially expressed genes associated with the branched-chain amino acids pathway. Genes that were differentially regulated (Fold change >= 2 and adjusted p-value <= 0.001) when Schizochytrium was cultured at 16 °C are indicated in red (upregulated) and blue (downregulated). Abbreviations: TAT: tyrosine aminotransferase; HGD: homogentisate 1,2-dioxygenase; FAH: fumarylacetoacetase; OXCT: 3-oxoacid CoA-transferase; ACCAT: acetyl-CoA C-acetyltransferase; BCATC: ketol-acid reductoisomerase; BCAT: branched-chain amino acid aminotransferase; BCKDH: 2-oxoisovalerate dehydrogenase E1 component; DBT: 2-oxoisovalerate dehydrogenase E2 component; ACAMD: acyl-CoA dehydrogenase; ECHS: enoyl-CoA hydratase; GCDH: glutaryl-CoA dehydrogenase; LEU: 3-isopropylmalate dehydratase; IVD: isovaleryl-CoA dehydrogenase; MCCB: 3-methylcrotonyl-CoA carboxylase beta subunit; HMGCS: hydroxymethylglutaryl-CoA synthase.

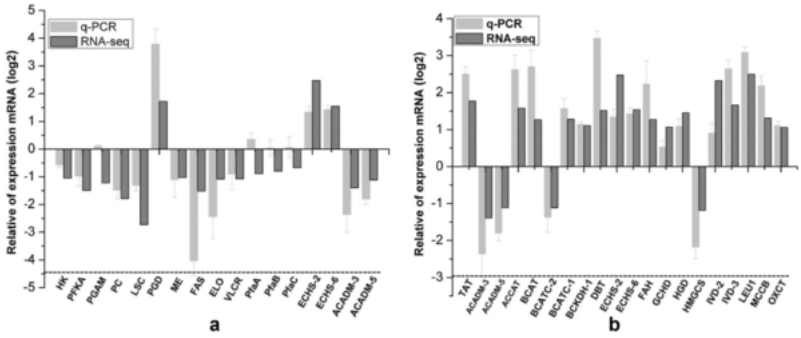

Figure 6

Transcriptomics and q-PCR analysis of the expression of genes involved in fatty acid metabolic pathway, glycolysis, the pentose phosphate pathway, the TCA cycle (a) and branched-chain amino acid degradation pathway (b). Positive and negative expression ratios represent up- and downregulation, respectively, in Schizochytrium sp. cultured at 16 °C. The results derived from q-PCR (light gray) were compared with those from transcriptomic analysis (black). HK: glycolysis hexokinase; PFKA: 6-phosphofructokinase; PGAM: phosphoglycerate mutase; PC: pyruvate carboxylase; LSC: succinyl-CoA synthetase; PGD: Glucose-6-phosphate 1-dehydrogenase; ME: malic enzyme; FAS: fatty acid synthase; ELO: long-chain fatty acid elongase; VLCR: very long-chain 3-oxoacyl-CoA reductase; PfaA: polyketide synthase subunit A; PfaB: polyketide synthase subunit B; PfaC: polyketide synthase subunit C; ACADM: acyl-CoA dehydrogenase; ECHS: enoyl-CoA hydratase. TAT: tyrosine aminotransferase; HGD: homogentisate 1,2-dioxygenase; FAH: fumarylacetoacetase; OXCT: 3-oxoacid CoA-transferase; ACCAT: acetyl-CoA C-acetyltransferase; BCATC: ketol-acid reductoisomerase; BCAT: branched-chain amino acid aminotransferase; BCKDH: 2-oxoisovalerate dehydrogenase E1 component; DBT: 2-oxoisovalerate dehydrogenase E2 component; ACADM: acyl-CoA dehydrogenase; ECHS: enoyl-CoA hydratase; GCDH: glutaryl-CoA dehydrogenase; LEU: 3-isopropylmalate dehydratase; IVD: isovaleryl-CoA dehydrogenase; MCCB: 3-methylcrotonyl-CoA carboxylase beta subunit; HMGCS: hydroxymethylglutaryl-CoA synthase.

Supplementary Files

This is a list of supplementary files associated with this preprint. Click to download.

- TableS3.docx
- TableS2.xlsx
- TableS1.docx
- TableS4.docx
- TableS5.docx